

Controlled Deposition of Silver Indium Sulfide Ternary Semiconductor Thin Films by Chemical Bath Deposition

Li-Hau Lin, Ching-Chen Wu, Chia-Hung Lai, and Tai-Chou Lee*

Department of Chemical Engineering, National Chung Cheng University, 168 University Road, Min-Hsiung, Chia-Yi 621, Taiwan

Received July 29, 2007. Revised Manuscript Received April 30, 2008

An aqueous method for the deposition of silver indium sulfide ternary semiconductor thin films is presented. According to grazing-incidence X-ray diffraction studies, a single phase of AgInS_2 with orthorhombic structure or a single phase of AgIn_5S_8 with cubic spinel structure can be selectively grown on 3-mercaptopropyl-trimethoxysilane-modified glass substrates. As-deposited thin films were annealed for 1 h in an argon environment at 400 °C in a tube furnace. It was found that when $[\text{Ag}]/[\text{In}] = 1$ in the precursor solution, AgInS_2 was obtained. On the other hand, AgIn_5S_8 resulted from $[\text{Ag}]/[\text{In}] \leq 0.33$ in the precursor solution. The energy gap, determined from transmission and reflection spectra, is located between 1.8 and 2.0 eV. The thickness of the thin films was in the range of 500–700 nm. Electrical resistivity was on the order of $10^4 \Omega\text{-cm}$. In addition, silver indium sulfide crystals were grown on octadecyltrichlorosilane-modified glass substrates without any post-thermal treatment. Powder X-ray diffraction and scanning electron microscope images indicated that crystalline AgIn_5S_8 aggregates were obtained. Detailed crystal structures, examined with a transmission electron microscope, electron diffraction, and high-resolution transmission electron microscope, further indicated that single crystals were prepared. According to these experimental findings, we were able to control compositions of silver indium sulfide thin films from aqueous solutions by suitable control of concentrations in the precursor solutions and surface functionalities. This technique provides an easy and cost-efficient way to deposit multicomponent semiconductor thin films.

Introduction

The I–III–VI ternary semiconductors with the chalcopyrite structure have useful applications in solar cells and optical devices.^{1–9} Both AgInS_2 ^{8,10–15} and AgIn_5S_8 ^{9,16–25} are promising materials, with the energy band gap in the range

of 1.7–2.0 eV.^{8–25} These two semiconductor materials can be prepared to have either n- or p-type conductivity and possess a resistivity between 10^2 and $10^6 \Omega\text{-cm}$, depending on the deposition methods.^{8–25} AgInS_2 has two major phases of tetragonal and orthorhombic structures. The tetragonal structure is presented below 620 °C, and it changes to the orthorhombic form above 620 °C.²⁶ On the other hand, AgIn_5S_8 has only the cubic spinel-type structure.²⁶ AgInS_2 or AgIn_5S_8 films on various substrates can be prepared by pulse laser vaporization,⁹ chemical spray pyrolysis,^{10–15} chemical bath deposition,^{16,17} vacuum evaporation,^{8,18–20} sulfurization of Ag–In alloy films,²¹ and aerosol-assisted chemical vapor deposition from a single precursor solution.^{22–25} Among these, evaporation and sulfurization methods have

* To whom correspondence should be addressed. Telephone: +886-5-2720411-33409. Fax: +886-5-2721206. E-mail: chmtcl@ccu.edu.tw.

- (1) Devaney, W. E.; Chen, W. S.; Stewart, J. M.; Mickelsen, R. A. *IEEE Trans. Electron Devices* **1990**, *37*, 428–433.
- (2) Basol, B. M.; Kapur, V. K. *IEEE Trans. Electron Devices* **1990**, *37*, 418–421.
- (3) Szot, J.; Prinz, U. *J. Appl. Phys.* **1989**, *66*, 6077–6083.
- (4) Wagner, S. *J. Appl. Phys.* **1974**, *45*, 246–251.
- (5) Fan, Y. X.; Eckardt, R. C.; Byer, R. L.; Route, R. K.; Feigelson, R. S. *Appl. Phys. Lett.* **1984**, *45*, 313–315.
- (6) Elsaesser, T.; Seilmeier, A.; Kaiser, W.; Koidl, P.; Brandt, G. *Appl. Phys. Lett.* **1984**, *44*, 383–385.
- (7) Eckardt, R. C.; Fan, Y. X.; Byer, R. L.; Marquardt, C. L.; Storm, M. E.; Esterowitz, L. *Appl. Phys. Lett.* **1986**, *49*, 608–610.
- (8) Hattori, K.; Akamatsu, K.; Kamegashira, N. *J. Appl. Phys.* **1992**, *71* (7), 3414–3418.
- (9) Bodnar, I. V.; Gremenok, V. F.; Rud, V. Yu.; Rud, Yu. V. *Semiconductors* **1999**, *33*, 740–743.
- (10) Gorska, M.; Beaulieu, R.; Loferski, J. J.; Roessler, B. *Thin Solid Films* **1980**, *67*, 341–345.
- (11) Ortega-Lopez, M.; Morales-Acevedo, A.; Solorza-Feria, O. *Thin Solid Films* **2001**, *385*, 120–125.
- (12) Ortega-Lopez, M.; Vigil-Galan, O.; Cruz Gandarilla, F.; Solorza-Feria, O. *Mater. Res. Bull.* **2003**, *38*, 55–61.
- (13) Albor Aguilera, M. L.; Ortega-Lopez, M.; Sanchez Resendiz, V. M.; Aguilar Hernandez, J.; Gonzalez Trujillo, M. A. *Mater. Sci. Eng., B* **2003**, *102*, 380–384.
- (14) Aissa, Z.; Ben Nasrallah, T.; Amlouk, M.; Bernede, J. C.; Belgacem, S. *Sol. Energy Mater. Sol. Cells* **2006**, *90*, 1136–1146.
- (15) Aissa, Z.; Amlouk, M.; Ben Nasrallah, T.; Bernede, J. C.; Belgacem, S. *Sol. Energy Mater. Sol. Cells* **2007**, *91*, 489–494.
- (16) Cheng, K.-W.; Huang, C.-M.; Pan, G.-T.; Chang, W.-S.; Lee, T.-C.; Yang, T. C. K. *J. Photochem. Photobiol. A: Chem.* **2007**, *190*, 77–87.

- (17) Lin, L.-H.; Wu, C.-C.; Lee, T.-C. *Cryst. Growth Des.* **2007**, *7*, 2725–2732.
- (18) Qasrawi, A. F.; Kayed, T. S.; Ercan, I. *Mater. Sci. Eng., B* **2004**, *113*, 73–78.
- (19) Konovalov, I.; Makhova, L.; Hesse, R.; Szargan, R. *Thin Solid Films* **2005**, *493*, 282–287.
- (20) Qasrawi, A. F. *J. Alloy. Compd.* **2007**, doi: 10.1016/j.jallcom.2007.01.030.
- (21) Makhova, L.; Szargan, R.; Konovalov, I. *Thin Solid Films* **2005**, *472*, 157–163.
- (22) Deivaraj, T. C.; Park, J.-H.; Afzaal, M.; O'Brien, P.; Vittal, J. J. *Chem. Commun.* **2001**, *22*, 2304–2305.
- (23) Vittal, J. J.; Deivaraj, T. C. *Prog. Cryst. Growth Charact. Mater.* **2002**, *45*, 21–27.
- (24) Deivaraj, T. C.; Park, J.-H.; Afzaal, M.; O'Brien, P.; Vittal, J. J. *Chem. Mater.* **2003**, *15*, 2383–2391.
- (25) Banger, K. K.; Jin, M. H.-C.; Harris, J. D.; Fanwich, P. E.; Hepp, A. F. *Inorg. Chem.* **2003**, *42*, 7713–7715.
- (26) Delgado, G.; Mora, A. J.; Pineda, C.; Tinoco, T. *Mater. Res. Bull.* **2001**, *36*, 2507–2517.

better control over the compositions of the films compared to solution-based techniques, such as spray pyrolysis and chemical bath deposition. However, the convenient experimental apparatus and the ability to grow larger films at a lower temperature make the solution growth processes attractive for industrial applications. Nevertheless, there are few reports in the literature which selectively prepare a single phase of AgInS_2 as well as a single phase of AgIn_5S_8 film from an aqueous solution by adjusting preparative parameters.¹⁰

In this report, chemical bath deposition was employed to deposit silver indium sulfide thin films on self-assembled monolayer (SAM)-modified glass substrates. The growth mechanism of binary compounds by chemical bath deposition has been studied extensively.^{27–30} The type and the concentration of complex agents and the degree of supersaturation play important roles in the heterogeneous nucleation on substrate surfaces from aqueous solutions. In our previous report,¹⁷ we studied the growth process of AgIn_5S_8 thin films on glass substrates by changing the pH, silver to indium concentration ratios $[\text{Ag}]/[\text{In}]$ of the precursor solutions, and post-thermal treatments. We found that, under our experimental conditions, a two-step growth mechanism was revealed: First, Ag_2S particles attached to the substrates. This seeding layer promoted the growth of In_2S_3 . After suitable thermal treatment, a uniform ternary semiconductor thin film was obtained. In addition, the surface property was also found to be another dominating factor. 3-Mercaptopropyl-trimethoxysilane (MPS)-modified glass substrates, having thiol functional groups exposed to the substrate surface, enhanced the adhesion and homogeneity of AgIn_5S_8 thin films. This prompted us to investigate the effects of surface functionalities on the thin film growth process, resulting in the controlled formation of uniform multicomponent thin films that have unique physical properties.

Recently, SAM-mediated depositions of biomineral materials,^{31–35} metal oxide,^{36–40} and metal sulfide^{41–46} have

been reported. The density of crystal nuclei differs from the types of the functional groups exposed to the surface, such as methyl ($-\text{CH}_3$), amine ($-\text{NH}_2$), carboxyl ($-\text{COOH}$), and mercaptan ($-\text{SH}$) terminated SAMs. These well-defined ω -functionalized SAMs can serve as a model system for studying the effects of surface properties on polymorph and nucleation faces of the crystals grown on the surface.⁴⁷ In this paper, we report the growth of silver indium sulfide thin films on SAM-modified glass substrates from aqueous precursor solutions. MPS and octadecyltrichlorosilane (OTS) were used to functionalize the glass surfaces. The main focus of this study is to show the controlled deposition of polycrystalline AgInS_2 and AgIn_5S_8 thin films. Furthermore, single-crystal AgIn_5S_8 aggregates can be grown also on SAMs generated from OTS without post-thermal treatment. Grazing-incidence X-ray diffraction (GIXRD), scanning electron microscopy (SEM), and transmission electron microscopy (TEM) were employed to study the crystal phase, surface morphology, and atomic-scale crystal organization of thin films and crystals obtained from various preparative factors.

Experimental Section

Materials. Analytical-grade silver nitrate ($\text{Ag}(\text{NO}_3)$), indium nitrate ($\text{In}(\text{NO}_3)_3 \cdot 5\text{H}_2\text{O}$), thioacetamide (CH_3CSNH_2 , TAA), triethanolamine ($(\text{HOCH}_2\text{H}_4)_3\text{N}$, TEA), sodium citrate ($\text{C}_6\text{H}_5\text{O}_7\text{Na}_3 \cdot 2\text{H}_2\text{O}$), citric acid ($\text{C}_6\text{H}_8\text{O}_7$), sulfuric acid (H_2SO_4), and ammonium nitrate (NH_4NO_3) were purchased commercially and used as-received. Aqueous cationic and anionic solutions were prepared separately before deposition. Glass substrates of 1 mm thick were cut into slides (1 cm \times 2 cm) and used immediately after cleaning to prevent further contamination on the surface. First, glass substrates were immersed in Piranha solution ($\text{H}_2\text{O}_2:\text{H}_2\text{SO}_4 = 3:7$) for 30 min and then rinsed thoroughly with deionized water. Substrates were then cleaned by subsequently soaking them in an ultrasonic bath in methanol, deionized water, and acetone for 10 min each, followed by thoroughly rinsing them with deionized water and blowing them dry with ultrapure nitrogen. Finally, the substrates were dried in an oven. The average roughness on either side of the glass substrate was 1.8 ± 0.3 nm after the cleaning process.

Surface Modification. Two types of SAMs were generated on glass substrates with different surface functionalities. The first type of self-assembled monolayer was derived from MPS (97%, Fluka) on the pre-cleaned glass substrate. A previous report provides a detailed preparation procedure, but a brief summary is given in this report.⁴⁸ The cleaned glass substrates were boiled in the solution (30% $\text{H}_2\text{O}_2:\text{NH}_4\text{OH}:\text{DI water} = 1:1:5$) at 80 °C for 30 min. The glass slides were rinsed with DI water and refluxed in a solution of 5 g of MPS in 30 mL of 25% isopropyl alcohol at 90 °C for 10

- (27) Han, S.-Y.; Lee, D.-H.; Chang, Y.-J.; Ryu, S.-O.; Lee, T.-J.; Chang, C.-H. *J. Electrochem. Soc.* **2006**, *153*, C382–C386.
 (28) Govender, K.; Boyle, D. S.; Kenway, P. B.; O'Brien, P. J. *Mater. Chem.* **2004**, *14*, 2575–2591.
 (29) Asenjo, B.; Chaparro, A. M.; Gutierrez, M. T.; Herrero, J.; Maffiotte, C. *Electrochim. Acta* **2004**, *49*, 737–744.
 (30) Yamaguchi, K.; Yoshida, T.; Lincot, D.; Minoura, H. *J. Phys. Chem. B* **2003**, *107*, 387–397.
 (31) Tang, R.; Darragh, M.; Orme, C. A.; Guan, X.; Hoyer, J. R.; Nancollas, G. H. *Angew. Chem., Int. Ed.* **2005**, *44*, 3698–3702.
 (32) Aizenberg, J.; Black, A. J.; Whitesides, G. M. *Nature* **1999**, *398*, 495–498.
 (33) Han, Y.-J.; Wysocki, L. M.; Thanawala, M. S.; Siegrist, T.; Aizenberg, J. *Angew. Chem., Int. Ed.* **2005**, *44*, 2386–2390.
 (34) Li, H.; Estroff, L. A. *J. Am. Chem. Soc.* **2007**, *129*, 5480–5483.
 (35) Toworfe, G. K.; Composto, R. J.; Shapiro, I. M.; Ducheyne, P. *Biomaterials* **2006**, *27*, 631–642.
 (36) Ritley, K. A.; Just, K.-P.; Schreiber, F.; Dosch, H.; Niesen, T. P.; Aldinger, F. *J. Mater. Res.* **2000**, *15*, 2706–2713.
 (37) Roddatis, V. V.; Su, D. S.; Beckmann, E.; Jentoft, F. C.; Braun, U.; Krohnert, J.; Schlogl, R. *Surf. Coat. Technol.* **2002**, *151–152*, 63–66.
 (38) Masuda, Y.; Sugiyama, T.; Seo, W.-S.; Koumoto, K. *Chem. Mater.* **2003**, *15*, 2469–2476.
 (39) Masuda, Y.; Kinoshita, N.; Sato, F.; Koumoto, K. *Cryst. Growth Des.* **2006**, *6*, 75–78.
 (40) Masuda, Y.; Yamagishi, M.; Koumoto, K. *Chem. Mater.* **2007**, *19*, 1002–1008.
 (41) Huang, L.; Zingaro, R. A.; Meyers, E. A.; Nair, P. K.; Nair, M. T. S. *Phosphorus, Sulfur Silicon Relat. Elem.* **1995**, *103*, 77–89.

- (42) Huang, L.; Zingaro, R. A.; Meyers, E. A.; Nair, P. K.; Nair, M. T. S. *Phosphorus, Sulfur Silicon Relat. Elem.* **1995**, *105*, 175–185.
 (43) Huang, L.; Nair, P. K.; Nair, M. T. S.; Zingaro, R. A.; Meyers, E. A. *Thin Solid Films* **1995**, *268*, 49–56.
 (44) LiuFu, S.-C.; Chen, L.-D.; Yao, Q.; Wang, C.-F. *J. Phys. Chem. B* **2006**, *110*, 24054–24061.
 (45) LiuFu, S.-C.; Chen, L.-D.; Wang, Q.; Yao, Q. *Cryst. Growth Des.* **2007**, *7*, 639–643.
 (46) Hwang, Y. K.; Woo, S. Y.; Lee, J. H.; Jung, D.-Y.; Kwon, Y.-U. *Chem. Mater.* **2000**, *12*, 2059–2063.
 (47) Love, J. C.; Estroff, L. A.; Kriebel, J. K.; Nuzzo, R. G.; Whitesides, G. M. *Chem. Rev.* **2005**, *105*, 1103–1169.
 (48) Heller, D. A.; Garga, V.; Kelleher, K. J.; Lee, T.-C.; Mahbubani, S.; Sigworth, L. A.; Lee, T. R.; Rea, M. A. *Biomaterials* **2005**, *26*, 883–889.

Table 1. Recipe of the Chemical Bath to Prepare Silver Indium Sulfide Thin Films on the Glass Substrate

solution	concentrations of the cationic chemical bath [M]				[Ag]/[In]
	silver	indium	TEA	citric acid	
A	0.026	0.026	0.37	0.064	1
B	0.026	0.013	0.37	0.064	2
C	0.026	0.0087	0.37	0.064	3
D	0.026	0.0065	0.37	0.064	4
E	0.026	0.0052	0.37	0.064	5
F	0.013	0.026	0.37	0.064	0.50
G	0.0087	0.026	0.37	0.064	0.33
H	0.0065	0.026	0.37	0.064	0.25
I	0.0052	0.026	0.37	0.064	0.20
J	0.026	0.026	0.185	0.064	1
K	0.026	0.026	0	0.064	1
L	0.0013	0.026	0.37	0.064	0.05

min. Finally, the SAM-coated glass substrates were removed from the solution, rinsed with DI water, and dried with a stream of nitrogen.

The second type of self-assembled monolayer, OTS (90%, Aldrich), was prepared on the precleaned glass substrate. Anhydrous iso-octane was used as the solvent. The substrates were dipped in 1 mM OTS for at least 6 h in a glove box. Finally, the SAM-coated glass substrates were removed from the solution, rinsed with iso-octane solvent, and dried with a stream of nitrogen.

Deposition of Silver Indium Sulfide Thin Films. The Ag–In–S thin films were prepared by chemical bath deposition. In this study, silver to indium concentration ratios [Ag]/[In] in precursor solutions were varied. The silver precursor ($\text{Ag}(\text{NO}_3)_3$ + TEA) and the indium precursor ($\text{In}(\text{NO}_3)_3$ + citric acid) were prepared separately. Prescribed concentrations of silver, indium, TEA, and citric acid were listed in Table 1. We also changed the concentration of TEA to investigate the impact of the amount of complex agent on the compositions of the final films. The acidity of the chemical bath was further adjusted by adding concentrated sulfuric acid. The two cationic solutions were stirred separately for 15 min; they were then mixed together and stirred for another 15 min, and finally thioacetamide (0.154 M) was added. The pH of the chemical bath was kept at pH 0.6 throughout this study. Precleaned glass substrates were mounted vertically into the precursor solution with a separation between each slide of 1 mm. The bath was placed on a hot plate with magnetic stirring. The reaction was carried out at 80 °C. After 1 h of deposition, the coated substrates were removed and cleaned. Following our previous report, postdeposition thermal treatment was performed in a vacuum tube furnace at 400 °C in an argon environment for 1 h after deposition on MPS-modified glass substrates. The thickness of the film was determined by SEM of a cross section. It is in the 500–700 nm range.

Characterization. Crystallographic study was carried out on a grazing-incidence X-ray diffractometer (GIXRD), Rigaku D/Max 2500, equipped with an 18 kW rotating anode X-ray generator. The incidence beam made an angle of 6° with the sample surface. The system includes focusing and parallel-beam optics, which provides alignment of the sample to the X-ray beams. The microstructure of the samples was studied by using a Hitachi S4800 field-emission scanning electron microscope (FE-SEM) and by using a Hitachi HF-2000 field-emission transmission electron microscope (TEM). EDX attached to FE-SEM was used to analyze the composition of the thin films qualitatively and electron diffraction (ED) of the crystals was conducted on TEM. Optical transmission and reflection spectra were recorded by a Shimadzu UV-2450 UV–vis spectrometer in the wavelength range from 300 to 900 nm. The electrical resistivity was measured by the four-probe method using an Elchema CM-308 conductometer. The samples were cut into a square of 1 cm × 1 cm and the experiment

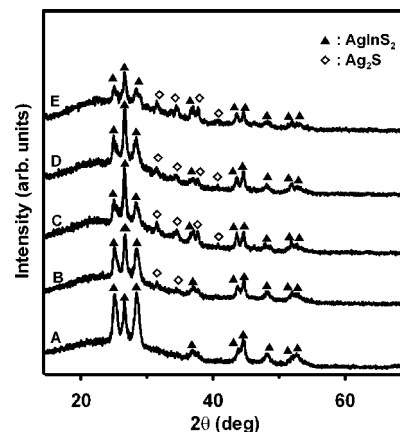


Figure 1. GIXRD patterns of samples prepared from precursor solutions on MPS-modified glass substrates after 1-h thermal treatment in an argon environment at 400 °C. (A) Solution A ([Ag]/[In] = 1), (B) solution B ([Ag]/[In] = 2), (C) solution C ([Ag]/[In] = 3), (D) solution D ([Ag]/[In] = 4), and (E) solution E ([Ag]/[In] = 5).

was conducted in a black box. The resistivity was obtained by averaging over three measurements for each sample and two samples for each experimental parameter.

Results

Thin Film Deposition on MPS-Modified Glass Substrate. The nucleation density and growth mechanism of I–III–VI ternary compounds are affected by the degree of supersaturation in the chemical bath. In addition, a self-assembled monolayer grown on the substrates provides another way to engineer surface properties for the preparation of various inorganic thin films. It has been shown that appropriate functionalities on the solid surface can promote heterogeneous nucleation on the substrate.⁴⁹ Our previous and preliminary work showed a two-step mechanism of AgIn_5S_8 thin film formation on glass substrates, in which Ag_2S particles attached to the surface first, followed by a uniform In_2S_3 deposition. The AgIn_5S_8 film grown on the MPS-modified substrate has a higher nucleation density and a better adhesion compared to that grown on a bare glass substrate.¹⁷ Based on these experimental findings, here in this study we investigate the AgInS_2 and AgIn_5S_8 thin film preparation by changing silver to indium concentration ratios [Ag]/[In] and concentrations of the complex agent, triethanolamine (TEA).

Grazing-incidence X-ray diffraction patterns shown in Figure 1 illustrate the silver indium sulfide ternary semiconductor thin film formation from an acidic solution (pH 0.6) with different silver to indium ratios. Concentrations of silver and thioacetamide (TAA) in the precursor solutions were kept the same (Table 1). The reaction was finished in 1 h. Under this experimental condition, a single phase of AgInS_2 thin film was obtained from solution A ([Ag]/[In] = 1), while the Ag_2S crystal phase appeared in addition to that of AgInS_2 with an increase in [Ag]/[In] from 2 to 5, corresponding to samples grown from solution B to solution E, respectively. The peaks marked with solid triangles are associated with reflections of the orthorhombic structure of AgInS_2 (JCPDS

(49) Gao, Y.; Koumoto, K. *Cryst. Growth Des.* **2005**, *5*, 1983–2017.

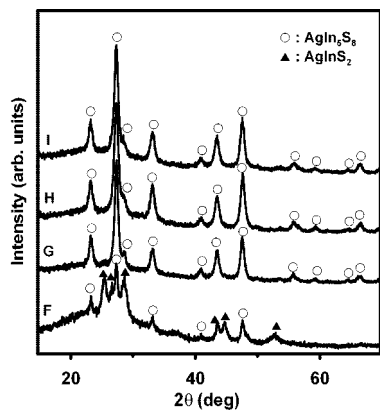


Figure 2. GIXRD patterns of samples prepared from precursor solutions on MPS-modified glass substrates after 1-h thermal treatment in an argon environment at 400 °C. (F) Solution F ([Ag]/[In] = 0.50), (G) solution G ([Ag]/[In] = 0.33), (H) solution H ([Ag]/[In] = 0.25), and (I) solution I ([Ag]/[In] = 0.20).

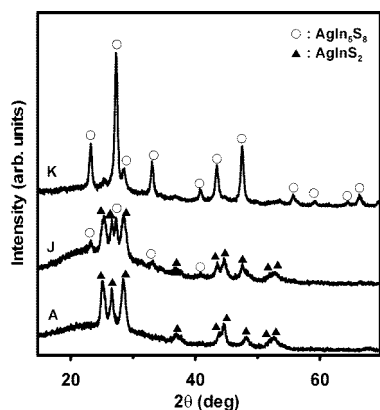


Figure 3. GIXRD patterns of samples prepared from precursor solutions on MPS-modified glass substrates after 1-h thermal treatment in an argon environment at 400 °C. (A) Solution A ([TEA] = 0.37 M), (J) solution J ([TEA] = 0.185 M), and (K) solution K ([TEA] = 0 M).

25-1328), and those marked with open diamonds can be ascribed to the monoclinic acantithe phase of Ag_2S (JCPDS 24-0072). On the other hand, if we kept the concentrations of indium and thioacetamide constant, a single-phase AgIn_5S_8 thin film of a cubic spinel structure (open circle, JCPDS 25-1329) results from a lower [Ag]/[In], shown in Figure 2. Throughout this paper, o- AgInS_2 and c- AgIn_5S_8 denote the orthorhombic phase of AgInS_2 and cubic phase of AgIn_5S_8 , respectively. Note that when [Ag]/[In] = 0.5, a mixture of o- AgInS_2 and c- AgIn_5S_8 can be clearly seen from the GIXRD patterns. Further decreases in [Ag]/[In] (solutions G, H, and I) eliminate the formation of the o- AgInS_2 crystal phase after thermal treatment, and only c- AgIn_5S_8 is presented. Next, we investigated the effect of TEA concentration on the phase change of the Ag–In–S system prepared from aqueous solutions. In the previous experiments, 0.37 M TEA was used as the complex agent for silver. It is observed that, in Figure 3, when the concentration of TEA was reduced to half (solution J) and to zero (solution K), the thin film with o- AgInS_2 prepared from solution A changes to a mixture of o- AgInS_2 and c- AgIn_5S_8 and to a single phase of c- AgIn_5S_8 , respectively. The grain size was further estimated by the Sherrer equation⁵⁰ for the (1 2 0) peak ($2\theta = 24.992^\circ$) and (4 0 0) peak ($2\theta = 33.064^\circ$) of AgInS_2 and AgIn_5S_8 ,

respectively. The particle sizes are 12.3, 11.4, and 16.9 nm for samples prepared from solution A, solution G, and solution K, respectively. Note that, at the angle of incidence in the GIXRD experiment, X-rays would probably penetrate the entire depth of the samples (500–700 nm), which, on the other hand, gives us enough information for phase identification. Theoretical and experimental investigations of the compositional depth profile were not sought in this study.

SEM images allow us to obtain information about the microstructure of sample surfaces. These micrographs (Figures 4a–c) reveal that the thin films prepared from aqueous solutions are rather dense and uniform. However, the surface morphologies are slightly different from sample to sample deposited under various conditions. Figure 4a shows the SEM image of the sample prepared from the precursor solution A. The crystal structure was determined to be o- AgInS_2 by GIXRD. The surface consists of a needle-like crystal network. When the silver to indium concentration ratio is reduced to 0.33 (solution G), the surface structure changes to collections of platelike aggregate (Figure 4b). Furthermore, a similar surface image is obtained for the sample prepared from the precursor solution K (Figure 4c). Both samples are of the c- AgIn_5S_8 crystal phase determined from GIXRD. It is observed that surface morphologies vary with a change in [Ag]/[In]. With higher silver to indium concentration ratio, [Ag]/[In] \geq 3, these needle-like crystallites coalesce to form granular clusters (Figure S1, Supporting Information), which is similar to that of the Ag excess AgInS_2 prepared from spray pyrolysis.¹⁴ On the other hand, at a lower silver to indium concentration ratio, [Ag]/[In] \leq 0.25, the film starts to form cracks observed at a lower magnification (10000 \times), as shown in Figure S2. The thicknesses of the films can further be determined from cross-section SEM images, shown in Figure 4d. This image corresponds to c- AgIn_5S_8 prepared from the precursor solution K (no TEA). From this image, the thickness is 615 nm. The thicknesses of the other two samples, o- AgInS_2 and c- AgIn_5S_8 deposited from precursor solutions A and G, are of the order of 498 and 687 nm, respectively.

EDX was employed to qualitatively analyze the compositions of the samples. The trend of the changes in compositions was studied on various [Ag]/[In] concentration ratios. Figure 5 plots the indium to silver atomic ratios presented in the thin films as a function of silver to indium concentration ratios in the precursor solutions. This figure is enlarged in the X-axis from 0 to 1 and Y-axis from 0 to 5 for a better illustration of the compositional changes during phase transformation from c- AgIn_5S_8 to o- AgInS_2 under different preparative conditions. According to the GIXRD investigation, thin films prepared from precursor solutions with [Ag]/[In] = 1 (solution A) and [Ag]/[In] = 0.33 (solution G) show a single phase of AgInS_2 and AgIn_5S_8 , respectively. In addition, when the precursor solution was set at [Ag]/[In] = 0.5 (solution F), a mixed-phase thin film was then obtained. The compositional analysis agrees well with the GIXRD result. It is seen that there is a kink at [Ag]/[In] = 0.5 on the figure. There are two straight lines, as guides for the eyes,

(50) Cullity, B. D. *Elements of X-ray Diffraction*; Addison Wesley: Reading, MA, 1978.

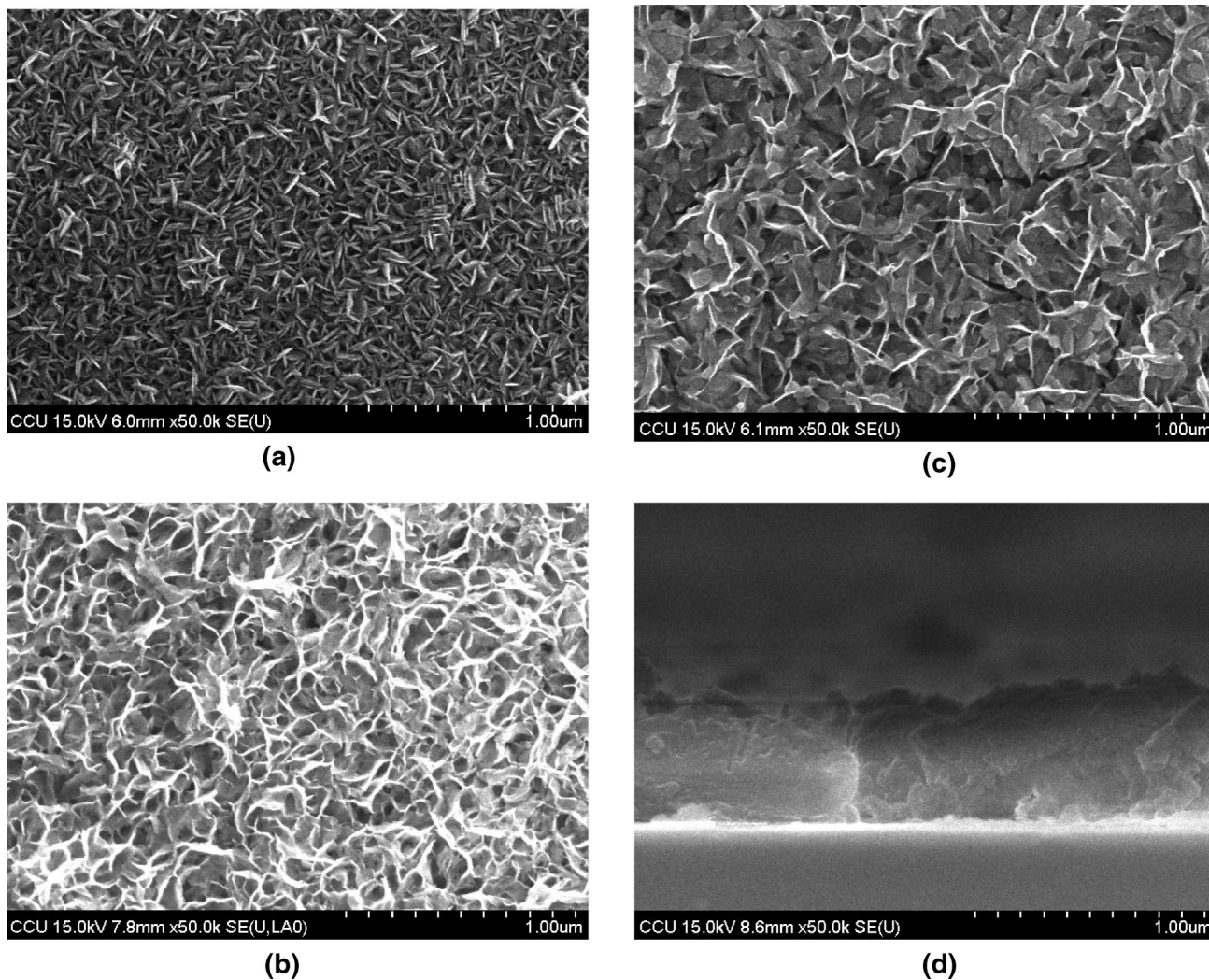


Figure 4. SEM micrographs of samples prepared from (a) solution A ([TEA] = 0.37 M), (b) solution G ([TEA] = 0.37 M), (c) solution K ([TEA] = 0 M), and (d) the cross-section image of the sample prepared from solution K.

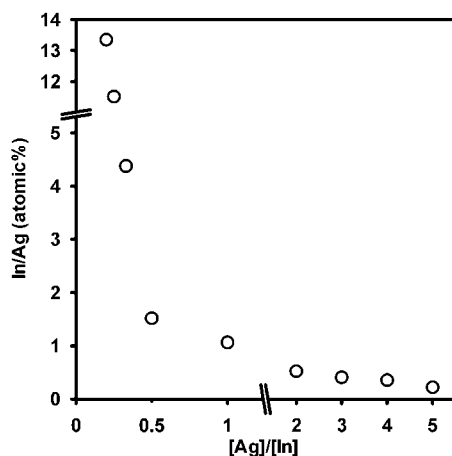


Figure 5. EDX elemental analysis of indium to silver atomic ratio presented in the thin films as a function of silver to indium concentration ratios in the precursor solutions.

above and below this point with different slopes, which suggests a different growth mechanism. More importantly, this result provides a way to control the compositions of silver indium sulfide ternary semiconductor thin films deposited on MPS-modified glass substrate.

We further examine the possibility to control the thickness of Ag–In–S ternary thin films by chemical bath deposition. According to the literature (e.g., refs 42 and 43), multiple dippings in the solution bath is one of the simple ways to adjust the thickness of the films. Based on our aforementioned findings, the compositions of the thin films can be controlled by suitable surface property and solution chemistry. AgIn_5S_8 prepared by CBD seems to have a wider operating window. Therefore, the MPS-modified glass substrate was dipped in solution G twice (GG) for 1 h each to increase the film thickness. Surprisingly, the powder XRD pattern (Figure S3a) shows that o-AgInS_2 is the major crystal phase, although the thickness increases to $1.20 \mu\text{m}$ determined by the SEM cross-section image. EDX analysis also shows that a silver-rich ternary sulfide was obtained ($\text{Ag}/\text{In}/\text{S} = 1:0.7:1.6$). We decreased the $[\text{Ag}]/[\text{In}]$ in the second precursor solution to 1/20 (solution L). The XRD pattern (Figure S3a) indicates that $\text{c-AgIn}_5\text{S}_8$ was obtained for the sample (GL) dipped in solution G first and then solution L for 1 h each. EDX analysis shows that $\text{Ag}/\text{In}/\text{S} = 1:5.2:8.7$, and the thickness of the thin film is averaged to be $1.75 \mu\text{m}$ (Figure S3b). It demonstrates that the thickness is also controllable by using chemical bath deposition.

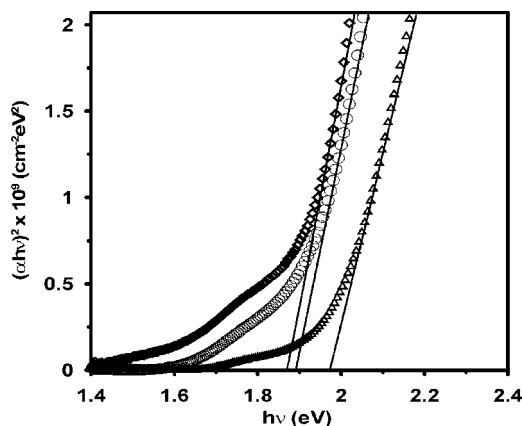


Figure 6. $(\alpha hv)^2$ vs hv plots for samples prepared from solution A (open diamond), solution G (open triangle), and solution K (open circle).

Optical transmission and reflection spectra were recorded by a UV-vis spectrometer in the wavelength range from 300 to 800 nm. The absorption coefficient α can be obtained from the following equation,⁵¹

$$T(\lambda) = [1 - R(\lambda)]^2 \exp(-\alpha d) \quad (1)$$

where $T(\lambda)$ and $R(\lambda)$ are transmittance and reflectance as a function of wavelength, respectively. d is the thickness of the film measured by SEM cross-section images. The transmission and reflection spectra are provided in the Supporting Information (Figure S4). Near the high-absorption region ($\alpha \geq 10^4 \text{ cm}^{-1}$), the absorption coefficient has the following frequency dependence:⁵¹

$$(\alpha hv) \approx (hv - E_g)^n \quad (2)$$

The absorption coefficient, α , can be obtained from eq 1. hv is the photon energy and n is a constant. Plot $(\alpha hv)^{1/n}$ with respect to hv and extrapolate the straight line to $(\alpha hv)^{1/n} = 0$, and thus the optical band gap is obtained. Generally, n is 2 for an indirect band gap and $1/2$ for a direct band gap. Figure 6 shows the linear dependence of $(\alpha hv)^{1/n}$ against hv when $n = 1/2$, which indicates a band to band transition. The optical energy gaps determined from optical measurement are in the range between 1.8 and 2.0 eV, where o-AgInS₂ (from solution A, open diamond) has the optical energy gap of 1.86 eV, and energy gaps of c-AgIn₅S₈ prepared from the precursor solution G (open triangle) and from precursor solution K (open circle) are 1.96 and 1.89 eV, respectively. The decrease of energy gap of c-AgIn₅S₈ (G and K) can be attributed to the increase of grain size, which was determined from X-ray diffraction (11.4 nm for G and 16.9 nm for K). In other semiconductor systems, the blue shift of the optical absorption for the films consisted of smaller particles results from the quantum confinement effects.⁵² Nevertheless, these values of the band gaps are in good agreement with those reported in the literature.⁹ Optical losses occurred at the longer wavelength away from the fundamental absorption

(Figure S4) might be due to the scattering of light by the grains and grain boundaries.⁵³

The room-temperature resistivities for chemically deposited films are on the order of $10^4 \text{ } \Omega\text{-cm}$. o-AgInS₂ (from solution A) has a resistivity of $3.85 \times 10^4 \text{ } \Omega\text{-cm}$, whereas c-AgIn₅S₈ (from solution G) and a mixture of AgInS₂/AgIn₅S₈ (from solution F) possess resistivities of 4.85×10^4 and $6.25 \times 10^4 \text{ } \Omega\text{-cm}$, respectively. These values also agree with those reported in the literature.^{8–25}

Crystal Growth on OTS-Modified Glass Substrate. The growth of silver indium sulfide on self-assembled octadecyltrichlorosilane monolayer-modified glass substrates was further investigated. An FT-IR spectrometer showed two strong absorption peaks at positions of 2848 and 2918 cm^{-1} by taking a clean glass substrate as the reference. These two values correspond to symmetric and asymmetric stretching of CH₂, respectively, which agree qualitatively with OTS SAMs reported elsewhere.⁵⁴ The average roughness of the surface after OTS modification was determined to be 2.1 nm by AFM. A static contact angle of 98° was measured by using water as the contact liquid. This value is lower than that of uniform OTS SAMs prepared on clean native silica substrates.⁵⁵ This discrepancy implies a partial coverage of OTS SAMs on glass substrate surfaces. However, the OTS-modified surface in this study is hydrophobic in general. We used this modified substrate to study the effects of a different surface functionality in the silver indium sulfide growth process.

The OTS-modified glass substrate was immersed in precursor solution A for 1 h. The resulting film was particulate and nonuniform judging by naked eye observation. The film was dried in a 100 °C oven for 30 min and no further thermal treatment was performed. Parts a–e in Figure 7 show a SEM micrograph, a powder X-ray diffraction pattern, a TEM image, an electron diffraction pattern, and a HRTEM image of the as-deposited sample, respectively. Surprisingly, although the film does not completely cover the surface, it appears as a coalescence of diamond-shaped crystallites as seen from the SEM image (Figure S5). In a certain region, even an individual particle with bipyramid morphology is observed (Figure 7a). The crystal structure recorded by powder XRD indicates a single-phase polycrystalline AgIn₅S₈ with the cubic spinel structure (Figure 7b). TEM, electron diffraction, and HRTEM were further employed to study the AgIn₅S₈ crystal structure on OTS SAMs. The crystals were collected on the TEM grid after sonicating the thin film samples in water for 1 h. The typical TEM image exhibits the polyhedron of the AgIn₅S₈ crystal (Figure 7c). Figure 7d illustrates the electron diffraction pattern of the whole crystal along the $[\bar{1}11]$ zone axis. The distinct spots are evidence of a single crystal of AgIn₅S₈. Moreover, a high-resolution TEM image was taken from the upper part of the AgIn₅S₈ crystal in Figure 7c along the same zone axis $[\bar{1}11]$. From the lattice image of the high-magnification HRTEM

(51) Pankove, J. I. *Optical Processes in Semiconductors*; Prentice-Hall, Inc.: Englewood Cliffs, NJ, 1971.

(52) Todorov, T.; Cordoncillo, E.; Sanchez-Royo, J. F.; Carda, J.; Escribano, P. *Chem. Mater.* **2006**, *18*, 3145–3150.

(53) Lai, F.; Li, M.; Wang, H.; Hu, H.; Wang, X.; Hou, J. G.; Song, Y.; Yousong, J. *Thin Solid Films* **2005**, *488*, 314–320.

(54) Kulkarni, S. A.; Mirji, S. A.; Mandale, A. B.; Gupta, R. P.; Vijayamohan, K. P. *Mater. Lett.* **2005**, *59*, 3890–3895.

(55) Wang, Y.; Lieberman, M. *Langmuir* **2003**, *19*, 1159–1167.

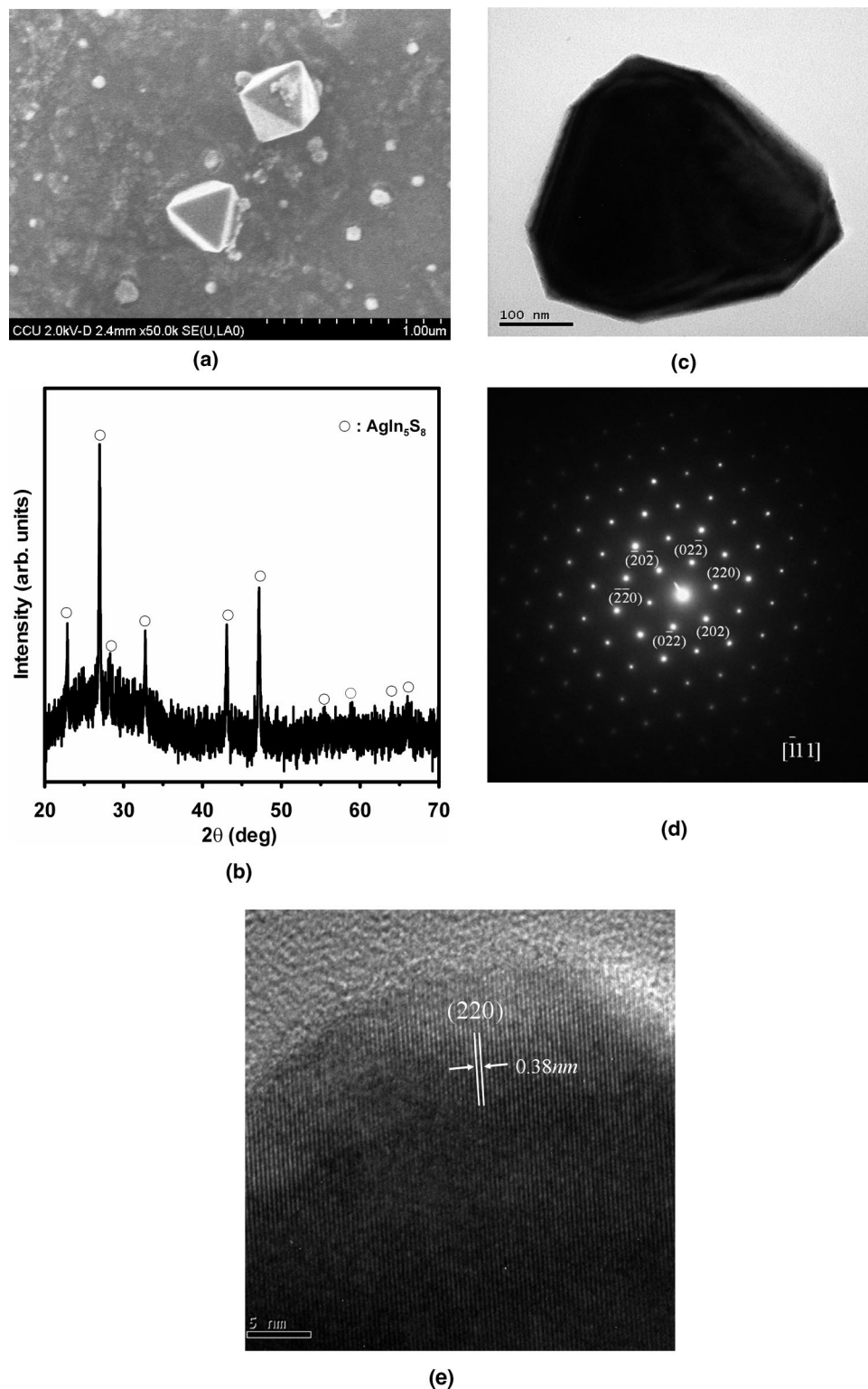


Figure 7. Sample prepared from solution A on OTS-modified glass substrates. (a) SEM micrograph, (b) powder XRD pattern, (c) low-magnification TEM image, (d) electron diffraction pattern of the whole grain, and (e) HRTEM image.

shown in Figure 7e, the lattice spacing of 0.38 nm is readily resolved, corresponding to the (2 2 0) crystal planes of the AgIn_5S_8 cubic spinel structure.

Discussion

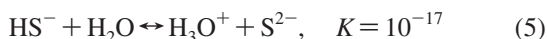
The ability to control the crystal phases of multicomponent semiconductor thin films is the key for industrial applications.

SAMs on substrate surfaces provide an environment to investigate the influences of surface properties on nucleation of solids from liquid phases.³² In this study, two types of SAMs, MPS and OTS, were generated on glass substrates. The major difference between these two SAMs is the surface functionality they provide after silanization and covalent bonding to the surface of the glass substrates. MPS has a

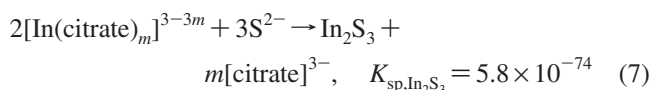
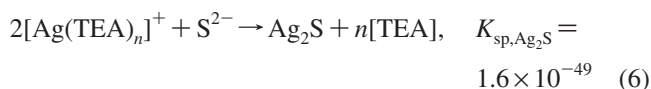
–SH tail group whereas OTS has a hydrophobic –CH₃ tail group. Upon heating of the precursor solution, the following reactions may occur:



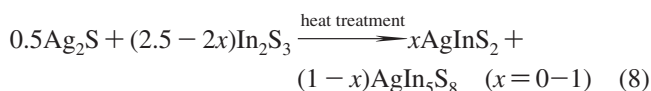
In an aqueous solution, H₂S dissociates to give



The predominant species in the solution will be HS[–] and the concentration of S^{2–} will be low. Silver and indium ions are complexed by the ligands. Solubility products (*K*_{sp}) of silver sulfide and indium sulfide are given by⁵⁶



In our previous study, it was found that Ag₂S particles were first deposited on the substrate surface and then In₂S₃ grew.¹⁷



The SAMs of MPS enhance the chemical affinity with silver,⁵⁷ resulting in a decrease in the interfacial tension, which promotes the heterogeneous nucleation on the surface. These densely packed Ag₂S particle aggregates provide the foundation for selective deposition of a single phase of AgInS₂ and AgIn₅S₈ crystalline thin films. An increase in the indium to silver atomic ratio in the films with an increase of [In]/[Ag] in the precursor solution is intuitively expected, but a slope change in Figure 5 is observed. Note that the experiments were conducted by fixing the silver concentration in precursor solutions while increasing [Ag]/[In] from [Ag]/[In] = 1. On the other hand, indium concentration was fixed in precursor solutions while decreasing [Ag]/[In] below [Ag]/[In] = 1. The change in slope at lower [Ag]/[In] values may be attributed to much fewer Ag₂S particles being deposited on the MPS-modified surface because of a lower degree of supersaturation. At the same time, the lower density Ag₂S clusters on the surface cause the crack formation under this experimental condition (Figure S2). The complex agent, TEA, also plays an interesting role. To the best of our knowledge, the stability constant of [Ag(citrate)_n]^{1–3n} and [In(TEA)_m]³⁺ could not be found in the literature.⁵⁶ According to our experimental findings (Figure 3), when the concentration of TEA is decreased, In/Ag in the thin films increases. This may be due to (1) a higher supersaturation of Ag₂S in the solution, less chelating agents bound to the silver cations, leading to a higher homogeneous nucleation density in the solution, and (2) redistribution of chelating

agents in the precursor solution, resulting in more free indium ions in the precursor. We examined the first layer formation by SEM (Figure S6). The average grain size of 50 nm is smaller than that of 100 nm prepared from the precursor solution A, as previously reported.¹⁷ In this two-step growth process, the first incubation and second incubation times for solution A are 10 and 50 min from the start of the reaction.¹⁷ However, without TEA as the chelating agent, the two incubation times shifted to around 5 and 30 min, respectively. It is expected that smaller Ag₂S particles deposit on the MPS-modified glass substrates and more In₂S₃ grows on top of the Ag₂S seeding layer, which leads to a higher In/Ag ratio in the films. In the end, c-AgIn₅S₈ thin films are obtained.

Additionally, high nucleation densities on the surface will produce a polycrystalline product, and a single crystal will be generated from a single nucleation site.⁵⁸ It is reasonable to grow polycrystalline AgIn₅S₈ and AgInS₂ thin films on MPS-modified glass substrates. Conversely, AgIn₅S₈ crystal aggregates were deposited on hydrophobic OTS-modified substrates without any post-thermal treatment. Figures S7a–S7c show the evolution of the crystal growth process on the OTS-modified substrate. These images were taken from the samples prepared from solution A on OTS-modified glass substrate for 30, 40, and 50 min, respectively. The initial layer consists of collections of particles and then the particles start to grow gradually. This time-dependent morphology evolution from cubic particles (Figure S7a) to the final aggregate of diamond-shapes crystals (Figure S5) can be observed. The compositions of the particles were determined by EDX (Figure S7d). Particles deposited for 30 min were primary Ag₂S (Ag/S = 1.80 and negligible In concentration). As the deposition continued, the concentration of indium increased. Finally, nearly stoichiometric AgIn₅S₈ was obtained after 1 h of reaction (Ag/In/S = 1:4.7:7.9). This figure also elucidates the two-step growth mechanism proposed. Note that the particle density of the first layer is much lower than that of the sample prepared on the MPS-modified glass substrate. Aizenberg et al. explained the localized crystallization on SAMs in terms of diffusion-limited and island-specific nucleation.³² In this scheme, they selectively created a rapidly nucleating region and a slowly nucleating region on the substrate surfaces. The rapidly nucleating region initiates the nucleation, induces ion flux to this region, and then creates a depletion zone of the reaction solution over the slowly nucleating region. Note that the contact angle of 98° implies the incomplete coverage of OTS SAMs. In the aforementioned model, single crystals grow at the edge of the island, where disordered SAMs are produced. Our silver indium sulfide growth on OTS SAMs can be considered analogous to this model. The closely packed OTS serves as the slow-growth region, and the loosely packed region of OTS SAMs and rough surfaces of the glass substrates provide the rapid-growth region. Ag₂S particles selectively attach to the rapid-growth region and offer the nucleation sites for In₂S₃ deposition. The second layer of In₂S₃ covers the Ag₂S first layer and then transforms to crystalline AgIn₅S₈.

(56) Perrin, D. D. *Stability Constants of Metal-Ion Complexes, Part B: Organic Ligands*; Pergamon Press: Oxford, 1979.

(57) Lam, K. F.; Yeung, K. L.; McKay, G. *Langmuir* **2006**, *22*, 9632–9641.

(58) Wucher, B.; Yue, W.; Kulak, A. N.; Meldrum, F. C. *Chem. Mater.* **2007**, *19*, 1111–1119.

Taking into account the Ag_2S – In_2S_3 phase diagram,⁵⁹ at a low deposition temperature (80 °C) and a low annealing temperature (400 °C), the following occurs: an evolution of Ag_2S , a mixture of Ag_2S and AgInS_2 , AgInS_2 , a mixture of AgInS_2 and AgIn_5S_8 , AgIn_5S_8 , and then to In_2S_3 from low to high In_2S_3 atomic percentage. According to this phase diagram, the window for AgInS_2 is slim. In other words, Ag_2S – AgInS_2 and AgInS_2 – AgIn_5S_8 coexistence phases appear more easily when the composition of this ternary compound is away from the stoichiometric ratio. On the other hand, the AgIn_5S_8 cubic spinel phase has a wide homogeneous region from 81 to 96 mol % In_2S_3 , corresponding to $\text{Ag}/\text{In} = 1:4.3$ and $1:24.0$, respectively. Therefore, a single-phase AgIn_5S_8 can be obtained by a wider range of $[\text{Ag}]/[\text{In}]$ precursor solutions, and a single-phase AgInS_2 can be obtained only by the $[\text{Ag}]/[\text{In}] = 1$ precursor solution under our experimental conditions. In the case of silver indium sulfide deposited on OTS-modified glass substrates, limited nucleation sites provide a chemical environment for the crystal growth. Thermodynamics determines the crystal phase of *c*- AgIn_5S_8 once the films contain more than 81% In_2S_3 . The multiple dipping experiments further show that the surface property and solution chemistry play important roles in the CBD process. With the same precursor solution, the composition of the films deposited on MPS- and OTS-modified glass substrates and the AgIn_5S_8 thin film surface are different. Nucleation density of the Ag_2S seeding layer also depends on the surface property. Different densities of Ag_2S seeding layers on modified glass substrates result in either polycrystalline thin films (on MPS-modified substrates) or single-crystal aggregates (on OTS-modified substrates). A suitable design of surface functionality and solution chemistry is expected to create novel structures for this ternary sulfide material.

Conclusions

In this study, two types of self-assembled monolayers were used to functionalize the glass substrate. These MPS- and OTS-modified glass substrates were employed to study the

silver indium sulfide deposition from an acidic aqueous solution. A single phase of AgInS_2 with the orthorhombic structure and a single phase of AgIn_5S_8 with the cubic spinel structure thin films can be selectively deposited on MPS-modified glass substrates under suitable preparative conditions after 400 °C thermal treatment. The grazing-incidence X-ray diffraction patterns revealed that a phase transformation from AgInS_2 to AgIn_5S_8 occurs when the precursor solutions vary from a higher $[\text{Ag}]/[\text{In}]$ to a lower $[\text{Ag}]/[\text{In}]$. Additionally, more TEA presented in the precursor solution promotes the growth of AgInS_2 , and no TEA in the precursor solution results in the formation of AgIn_5S_8 thin films. The EDX compositional analysis agreed with the trend of the GIXRD results qualitatively. The films obtained from this work are rather adherent and uniform, as observed from the SEM images. The optical band gaps determined from transmission and reflection spectra of the thin-film samples are in the range of 1.8 and 2.0 eV, where *o*- AgInS_2 (from solution A) has the energy gap of 1.86 eV, and energy gaps of *c*- AgIn_5S_8 prepared from the precursor solution G, and from precursor solution K are 1.96 and 1.89 eV, respectively. On the other hand, silver indium sulfide deposition on OTS-modified glass substrates showed *c*- AgIn_5S_8 crystalline aggregates without any thermal treatment. TEM, HRTEM, and ED indicated that each crystal is single crystal. The selective deposition mechanism was used to explain our experimental results. More importantly, this study demonstrates the ability to control the compositions of the multi-component semiconductor thin films as well as the crystal growth on suitable engineered substrate surfaces.

Acknowledgment. This work was supported by the National Science Council of Taiwan (Grant No. NSC 95-2221-E-194-082). We thank the Instrument Centers for assistance with SEM micrographs (National Chung Cheng University), GIXRD analysis (National Cheng Kung University), and TEM images (National Cheng Kung University).

Supporting Information Available: SEM images, powder XRD patterns, transmission, and reflection spectra of Ag–In–S ternary semiconductor thin films prepared under various experimental conditions (PDF). This material is available free of charge via the Internet at <http://pubs.acs.org>.

CM702081H

(59) Sachanyuk, V. P.; Gorgut, G. P.; Atuchin, V. V.; Olekseyuk, I. D.; Parasyuk, O. V. *J. Alloy. Compd.* **2008**, *452*, 348–358.